PHYSICAL REVIEW A VOLUME 43, NUMBER 4 15 FEBRUARY 1991

# Monte Carlo study of CO oxidation on an anisotropic surface

B. Yu and D. A. Browne
*Department of Physics and Astronomy, Louisiana State University, Baton Rouge, Louisiana 70803-4001*

P. Kleban
*Department of Physics and Astronomy, and Laboratory for Surface Science and Technology, University of Maine, Orono, Maine 04469*

(Received 18 June 1990)

It is well established that anisotropy does not affect the critical behavior of a system in thermodynamic equilibrium that undergoes a second-order phase transition. We study here an anisotropic kinetic model for heterogeneous catalysis that mimics the oxidation of CO on the (110) surface of a transition metal like Pd. We have mapped out the phase diagram of possible steady states for various anisotropic reaction and absorption processes as a function of the $O_2$/CO adsorption rate and the CO diffusion rate. The phase diagram depends upon the amount of anisotropy and exhibits both a first-order and a second-order phase transition for a reactive to an unreactive steady state. We have examined the critical behavior at the second-order phase transition with finite-size scaling and have found that this model belongs to the directed percolation universality class irrespective of the anisotropy.

## I. INTRODUCTION

Over the past 25 years, much theoretical and experimental effort has gone into understanding the properties of a system in thermodynamic equilibrium as it undergoes a phase transition. The critical behavior near a second-order transition has attracted particular attention[1] because the mean-field description breaks down near the transition due to the presence of large fluctuations associated with the change in the symmetry properties of the thermodynamic state. The critical behavior shows "universal" properties in the sense that the critical exponents which describe the behavior near the transition are essentially independent of the microscopic details, and depend only on the spatial dimensionality and the symmetry properties of the Hamiltonian. In conjunction with theoretical tools like the renormalization group,[1] these ideas of scale invariance and coupling of fluctuations on all length scales have developed into a simple and elegant picture of the long-wavelength and low-frequency behavior of a system in equilibrium near a phase transition.

There is a larger class of physical systems consisting of many degrees of freedom whose steady state is not described by thermodynamic equilibrium. These are often open systems driven by an external force, and examples are found in exciton dynamics[2] and chemical reactions.[3] The dynamical evolution of these nonequilibrium systems is often given by specifying a set of kinetic rules that describe a single step in the evolution of the state of the system. The kinetic rules generally do not obey detailed balance. For example, a system may undergo an irreversible process for which the reverse process is forbidden. Even though these dynamical systems do not attain thermodynamic equilibrium, under rather general conditions they do reach a macroscopic steady state. Like an equilibrium system, these systems can also undergo a "phase transition." We use the term loosely here since it does not have the usual meaning of singular behavior in the free energy. Rather, we mean simply that as various rate parameters are changed in a smooth fashion, the macroscopic steady state undergoes singular changes. For example, in a chemical reaction system the reactant concentration could change discontinuously (a first-order phase transition) or continuously (a second-order phase transition). Compared to systems in equilibrium, relatively little is known about the nature of kinetic phase transitions in these systems, particularly as to the kinds of universality classes and what features of a given model determine the universality class.

In this paper, we will study the effect of spatial anisotropy on the phase diagram and the critical properties of one such kinetic model. It is well established that the asymptotic critical behavior of a system in thermal equilibrium is not affected by spatial anisotropy, although it can lead to crossover effects close to the transition as the effective dimensionality of the critical fluctuations changes. We want to see if the same holds true in a nonequilibrium kinetic model. The model we will study describes a nonequilibrium chemical reaction, and is an extension of a model studied by Ziff, Gulari, and Barshad[4] (ZGB) for the catalytic oxidation of CO on a transition metal surface.

In the ZGB model the surface is modeled as a square lattice of sites which can be occupied either by a CO molecule or an oxygen atom. A mixture of CO and $O_2$

 

gas is fed to the surface where the oxidation of CO to produce $CO_2$ occurs. It takes one vacant site to adsorb a CO molecule, and it takes two neighboring empty sites to adsorb an $O_2$ molecule. The adsorption of an $O_2$ molecule can be in either the $\hat{\mathbf{x}}$ or $\hat{\mathbf{y}}$ direction with equal probability. The reaction occurs if O and CO are nearest neighbors, and the reaction rate is independent of the orientation of the pair of reactants. Diffusion and desorption of the reactants is ignored, and the desorption of the product is assumed to be instantaneous. The adsorption of the reactants is the bottleneck in the ZGB model and a single free parameter $y_{CO}$, the mixing ratio of CO and $O_2$ gas, is the only control parameter. As this parameter varies, the steady-state coverage of CO and O coverage changes. Therefore one can map out a phase diagram of CO and O coverage as a function of $y_{CO}$.

Ziff, Gulari, and Barshad[4] found through simulations on a 128 × 256 lattice that their model exhibits two nonequilibrium phase transitions. There are two absorbing states (states that cannot be left once they are entered), corresponding to saturation of the surface by one reactant, in addition to a reactive steady state. For $y_{CO} < y_1 \approx 0.389$ the adsorbing state corresponds to a surface saturated by oxygen. The other adsorbing state, a surface entirely covered by CO, occurs for $y_{CO} > y_2 \approx 0.527$. Between $y_1$ and $y_2$, a reactive steady-state region exists where the surface is only partially occupied by CO and O, and the $CO_2$ formation rate assumes a nonzero value. As $y_{CO}$ increases past $y_1$, the steady state changes from the O saturated state to the reactive steady state via a second-order phase transition. The reactive steady state is replaced by the CO saturated state via a first order phase transition at $y_{CO} = y_2$.

The ZGB model was studied by Dickman using a mean-field approach[5] that approximates the kinetic equations for the spatial correlations by truncating the correlations at a certain range. At the level of ignoring pair and higher-order correlations the equations are the same as the usual Langmuir adsorption equations with a Langmuir-Hinshelwood reaction term. His method correctly predicted the qualitative features of the phase diagram with two adsorbing states and a reactive steady state, although the positions of transitions were somewhat in error. Dickman found better results by including nearest-neighbor correlations, with[5] a first-order transition at $y_{CO} = 0.56$ and a second-order transition at $y_{CO} = 0.25$.

Meakin and Scalapino[6] reproduced the ZGB results with a larger square lattice of 512 × 512 and also on a hexagonal lattice of 512 × 512. The essential features of the phase diagram of square lattice remain unchanged in the hexagonal lattice except the first-order phase transition occurs at $y_{CO} = 0.561$ and the second-order phase transition occurs at $y_{CO} = 0.344$. Meakin and Scalapino[6] estimated that near the second-order transition the CO coverage varied as $N_{CO} \propto (y - 0.344)^{\beta_{CO}}$, with a critical exponent $\beta_{CO} \approx 0.69$. Similarly they found the oxygen coverage obeyed $1 - N_O \propto (y - 0.344)^{\beta_O}$, with $\beta_O \approx 0.61$. From their work they could not rule out the possibility of the exponents being the same. Grinstein, Lai, and Browne[7] argued from a simple renormalization-group approach and some numerical simulations that the ZGB model belongs to the universality class of Reggeon field theory[8] and directed percolation,[9] for which the critical exponent $\beta$ is 0.58. The continuous transition in a kinetic model to a noiseless (absorbing) state is generally believed[7,10] to be in this universality class. Extensive simulations by Jensen, Fogedby, and Dickman[11] have confirmed that the dynamic behavior of the ZGB model belongs to universality class of Reggeon field theory and directed percolation.

The oxidation of CO has been studied extensively experimentally and has been the subject of numerous theoretical papers besides those mentioned above. Much recent work has been directed towards improving the mean-field rate equations to account for the local correlations that are needed to correctly describe the $O_2$ adsorption and the $CO_2$ reaction. Dumont, Poriaux, and Dagonnier[12] studied a model similar to the ZGB model but with a finite $CO_2$ production rate. They used simulations to correct the coverage dependence of the mean-field adsorption and reaction rates. Their work was extended by Araya *et al.*[13] to include CO desorption and the effect of having several choices for potential partners to react with and having several neighboring vacancies when considering $O_2$ desorption. Their work was further extended by Ehsasi *et al.*[14] and by Kaukonen and Nieminen[15] to include CO diffusion. These latter authors also examined the influence of local adatom interactions[16] on changing the adsorption, desorption, reaction, and diffusion rates. The conclusion one reaches is that the qualitative features of the simplified ZGB model are not essentially changed by using a more realistic model. One feature that has not yet been explored is the effect of anisotropy, which is the subject of this paper.

The paper is organized in the following manner. In Sec. II we discuss the model and our simulation technique. The results we obtained for the phase diagram and the critical behavior are presented in Sec. III, and Sec. IV contains discussion and conclusions.

## II. ANISOTROPIC REACTION MODEL

The present model was motivated largely by structural anisotropy of the (110) surface of Pd. Pd has a fcc crystal structure, and if the crystal is cut along a (110) plane the surface appears to have rows of elevated atoms in the [001] direction, as shown in Fig. 1. We will call the [001] and $[1\bar{1}0]$ directions the $\hat{\mathbf{x}}$ and $\hat{\mathbf{y}}$ directions, respectively. Since the geometry in the two directions is different, it is reasonable to assume that adsorption and reaction processes will occur at different rates along each direction. Therefore we incorporated anisotropy into the kinetic rules to simulate the structural anisotropy. By studying the critical behavior of this anisotropic model, we will be able to determine whether anisotropy affects the universality class for the critical behavior of this nonequilibrium phase transition.

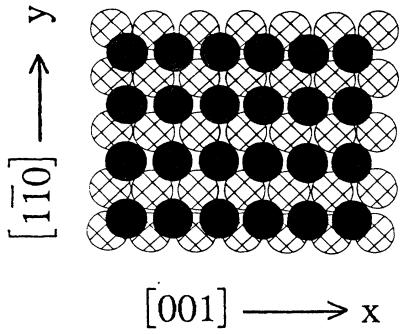


FIG. 1. Structure of the (110) surface of a fcc crystal. The solid circles denote top layer atoms and the cross-hatched circles show the locations of the second layer atoms.

We introduced anisotropy into both the adsorption and reaction rules. We assume that the adsorption of $O_2$ requires two adjacent sites, as in the ZGB model, but we will assume the $O_2$ molecule can be adsorbed only when oriented along the $\hat{\mathbf{y}}$ direction, that is, perpendicular to the troughs. No adsorption is permitted for molecules oriented along the trough even if there are two empty sites available. The choice of the $\hat{\mathbf{y}}$ direction for adsorption is completely arbitrary; the essential point is to permit adsorption only in one direction. We also will assume that the reaction of CO and O depends on whether the reactants are in the same trough or in adjacent troughs. We will call the probability to react in the same trough (perpendicular the $O_2$ adsorption direction) $R_x$, the probability of reacting when the reactants are in adjacent troughs is denoted $R_y = 1 - R_x$.

In our simulations, one Monte Carlo trial for the adsorption and reaction process is performed as follows. An empty site is chosen at random and then a molecule is chosen to adsorb, either a CO is chosen with probability $y_{CO}$ or an $O_2$ with probability $1-y_{CO}$. If a CO is chosen, it will immediately react if any of the four neighboring sites are occupied by O. If the CO can react with more than one O, the reaction probability for a given direction ($\hat{\mathbf{x}}$ or $\hat{\mathbf{y}}$) is weighted by $R_x$ or $R_y$. Once the reacting partner is chosen, the reaction is instantaneous and both the CO and O are removed from the surface. If the adsorbing molecule is $O_2$, one of the two nearest neighbors in the $\hat{\mathbf{y}}$ direction is chosen at random with equal probability. If this second site is empty, the $O_2$ is adsorbed, and the six nearest neighbors are immediately searched for CO molecules to react with and the reaction proceeds in the same manner as described for CO adsorption events.

In order to model the system more realistically, we also considered the possibility of CO diffusion on the surface. We did not include oxygen diffusion because experiments show[17] that it does not diffuse easily on the Pd surface due to its large binding energy. In each diffusion cycle, one CO is picked at random and one of its four nearest-neighboring sites is chosen with equal probability. If the site chosen is empty, the CO is moved to that site and the three neighbors are checked to see if a reaction is possible according to the rules described above. If so, $CO_2$ is formed and removed from the surface. This cycle is repeated a total of $R_d$ times for each adsorption and reaction cycle, where $R_d$ is the diffusion rate. For example, if the diffusion rate is ten times faster than the reaction rate, after each reaction cycle ten CO molecules on the surface will be selected for diffusion. In the algorithm, it is possible for one CO to be picked repeatedly.

Except for the finite-size scaling analysis described later, our simulations were done on a 100 x 100 square lattice starting from an empty lattice. The basic time unit in the simulation is one Monte Carlo step (MCS), which is defined as one Monte Carlo trial for adsorption and reaction for every site of the lattice. Each run was "thermalized" for 2000 MCS's and data were taken for the following 3000 MCS's to determine the steady-state properties. In addition to the parameter $y_{CO}$ in the ZGB model, we have as parameters the reaction probability along the trough $R_x$, and the CO diffusion rate $R_d$. In this model, if we permitted $O_2$ adsorption in both directions, set $R_x = R_y$, and ignored diffusion, we would recover the ZGB model.

## III. RESULTS

### A. Phase diagram with no diffusion

Figure 2 shows the O coverage on the lattice versus $y_{CO}$ for various values of $R_x$ with no diffusion. The first- and second-order phase transitions present in the ZGB model appear here as well, although the position of the transition and the behavior of the coverage near it depends on $R_x$. In Fig. 2 there is no obvious shift of the

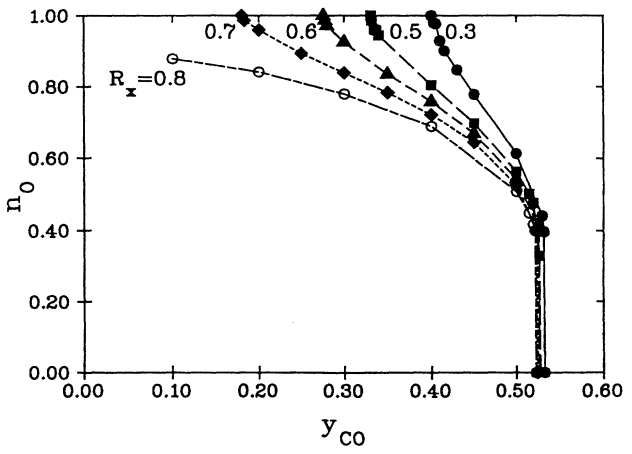


FIG. 2. Oxygen coverage $n_O$ vs $y_{CO}$ for various values of $R_x$ for a 100 x 100 lattice. Note that while the position of the second-order transition is very sensitive to the value of $R_x$, the first-order transition moves very little.

first-order transition with $R_x$, but a closer examination reveals a linear dependence of the transition point with $R_x$ as shown in Fig. 3. A least-squares fit to the data gives a slope of $0.02 \pm 0.0008$.

On the other hand, the location of the second-order phase transition is quite sensitive to the value of $R_x$. As $R_x$ increases, the position of the second-order phase transition $y_1$ shifts to lower values, suggesting that the surface becomes harder to saturate with oxygen. The shift of $y_1$ does not obey the linear relationship seen for $y_2$. The second-order transition disappears smoothly at $R_x = 0.742 \pm 0.002$, and the larger values of $R_x$ the reactive steady state appears to be present for $0 < y_{CO} < y_2$ as shown in Fig. 4.

Between the first- and second-order transitions, the phase diagram of Fig. 2 shows a reactive steady state similar to that seen in the ZGB model. For fixed $y_{CO}$, the O coverage of the surface decreases with increasing $R_x$. The CO coverage stays very low throughout the reactive steady-state region and the surface consists primarily of adsorbed O and vacancies.

Much of the behavior can be explained by recalling that in this model the $O_2$ can only be adsorbed in the $\hat{y}$ direction. The reaction rate $R_y$ measures the rate for creating a pair of vacant sites along the $\hat{y}$ direction. It is only these pairs of sites on which an $O_2$ molecule can adsorb. Near the second-order phase transition, the surface is nearly completely covered by O and most vacant sites are isolated. In order for an isolated site to be occupied by $O_2$, a CO molecule must adsorb and react in the $\hat{y}$ direction to create a pair of vacant sites for $O_2$ adsorption. If $R_y$ is large, it is quite likely that such a pair will be created, favoring $O_2$ adsorption. Therefore the system is more easily saturated with oxygen, which is consistent with the phase diagram. As $R_x$ decreases ($R_y$ increases), the second-order transition shifts towards higher values of $y_{CO}$ (less $O_2$), indicating that a larger CO adsorption rate is needed to prevent the surface from saturating with oxygen.

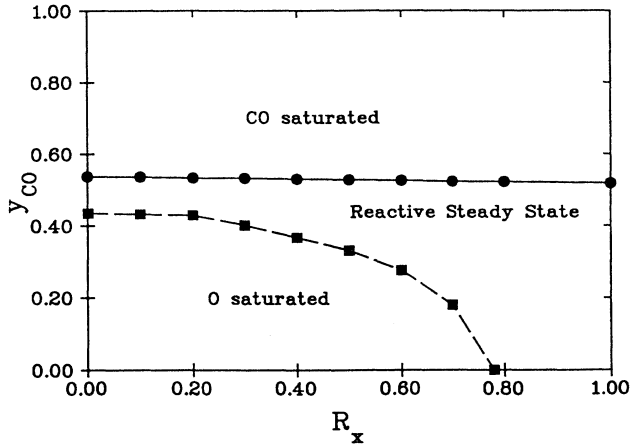


FIG. 4. The phase diagram for this model with no CO diffusion as a function of $y_{CO}$ and $R_x$.

On the other hand, near the first-order transition, the lattice is almost half vacant. Many vertical pairs of vacant sites already exist. Increasing $R_y$ does not significantly increase the likelihood of $O_2$ adsorption through the process of creating pairs of vacant sites along the $\hat{y}$ direction. Hence increasing $R_y$ is not very effective in suppressing the saturation of the surface with CO and so $y_2$ only increases slightly as $R_y$ increases.

### B. Behavior with diffusion

Figure 5 shows that for a given $R_x$, no significant shift of the first-order transition point $y_2$ occurs until the diffusion rate $R_d$ is comparable to the net reaction rate. For $R_d \geq 1$, $y_2$ shifts towards larger values of $y_{CO}$. Diffusion not only affects $y_2$, it also changes the magnitude of the jump, which shrinks as the diffusion rate increases. This behavior was also noted in simulations of the ZGB

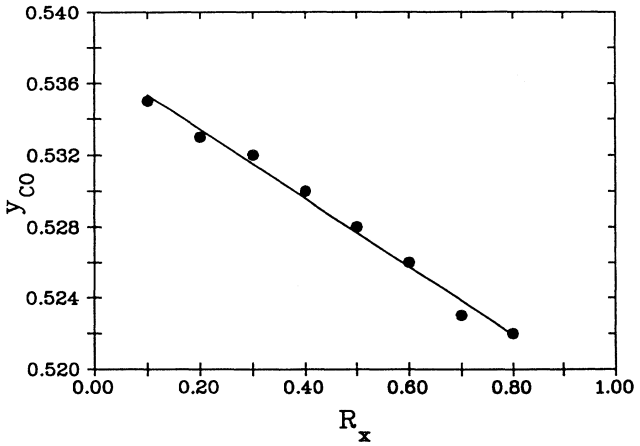


FIG. 3. The location of the first-order transition $y_2$ vs $R_x$. Note the greatly expanded scale along the ordinate.

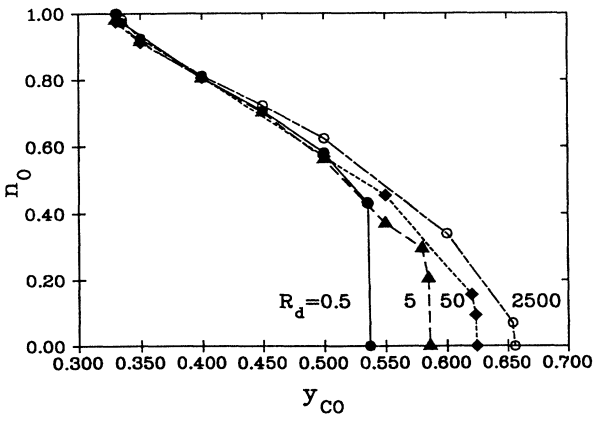


FIG. 5. Oxygen coverage $n_O$ vs $y_{CO}$ for various diffusion rates with $R_x = 0.25$ on a $100 \times 100$ lattice.

model with diffusion by Kaukonen and Nieminen[15] and by Ehsasi *et al.*[14] For $R_d \to \infty$ the transition to the CO saturated surface appears to be continuous.

The second-order transition point $y_1$ is quite insensitive to the diffusion rate $R_d$ as shown in Fig. 5. This happens in part because each CO must be surrounded by four vacancies, but the vacancy fraction vanishes at the transition. In addition, the diffusion of CO tends to make it more reactive by allowing it to move next to an O and react, which helps deplete the surface of CO. Hence there is no CO present to diffuse as $y_{CO} \to y_1$. Further away from the second-order transition, the diffusion does increase the steady-state O coverage slightly, as the above argument would imply.

Near the first-order phase transition, however, the CO concentration on the surface is much higher and small islands of CO appear on the surface. The diffusion of CO tends to break up these islands and prevent them from coalescing and eventually saturating the surface. A higher value of $y_{CO}$ is needed to adsorb more CO to offset this dispersal process. Diffusion also makes the CO more reactive by allowing it to move about and seek out an adsorbed oxygen to react with. This tends to reduce the steady-state CO concentration on the surface for a given value of $y_{CO}$. This effect must be offset by a higher $y_{CO}$ in order to saturate the surface, therefore the critical point $y_2$ shifts towards larger values.

### C. One-dimensional adsorption and reaction

There are two limiting cases where different rows of the lattice are decoupled and the behavior on the two-dimensional lattice appears one dimensional in character. The first case appears in the limit of $y_{CO} \to 0$, where there is no reaction and the surface is randomly populated by $O_2$ molecules. Each row in the $\hat{\mathbf{y}}$ direction is independent and the addition of $O_2$ molecules to a given row is equivalent to a model for random adsorption of dimers on a one-dimensional chain. The dimer coverage for such a problem is known[18] to be $1 - e^{-2} = 0.864\,664\ldots$, and our simulation in this limit gave a result of 0.8636.

The other limiting case appears for $R_x \equiv 1$. Here there is no possibility of reaction between adjacent troughs to create the pairs of vacant sites that the oxygen molecules need to adsorb. We find that in this limit there is no reactive steady state. Instead, two different absorbing states appear as $y_{CO}$ changes. For $y_{CO} > y_2$, where $y_2$ is the smoothly extrapolated value for $R_x \to 1$, the steady state consists of a surface saturated with CO as before. For $y_{CO} < y_2$, this state is replaced with one consisting of rows of both CO and O oriented along the $\hat{\mathbf{x}}$ direction, with all sites filled. In this steady state it is not possible for both species to coexist in the same trough, and the only stable configuration for a row is to be populated by a single species. This is akin to $A + B \to AB$ reactions in one dimension, which exhibit only $A$- or $B$-saturated states.[4,6] As $y_{CO}$ changes, the only possible change of configuration is to replace a row of one species with a row of another. In a finite system this leads to jumps in coverage as $y_{CO}$ varies. The jumps disappear in the limit of an infinite system. Interestingly, we find there is no correlation in the spatial distribution of CO and O rows, even though the $O_2$ adsorption must occur in adjacent troughs. The third possibility, an O-saturated surface, is ruled out because it occurs only at $Y_{CO} = 0$, which is the dimer-packing limit mentioned above.

### D. Critical behavior

As we noted earlier, there is considerable evidence[7,11] that the critical behavior near the second-order transition in the ZGB model belongs to the same universality class as Reggeon field theory and directed percolation. As we saw from the phase diagram in Fig. 4, the position of the second-order phase transition depends upon $R_x$. For $R_x \geq 0.742$, the second-order transition disappears. This behavior is akin to a shift in transition temperature in an equilibrium system with anisotropy. It is interesting therefore to ask whether the critical behavior is also affected by anisotropy.

We investigated the critical behavior of the second-order phase transition by using finite-size scaling to obtain the critical exponents. In the present study we examined two exponents, one for the static behavior and one for the dynamics.

For the static behavior we studied the critical exponent $\beta$ that describes the behavior of the "order parameter" $\psi$, which we chose to be the fraction of sites not occupied by O atoms: $\psi = 1 - n_O$. Because of the very low CO coverage, this order parameter really measures the vacancy fraction. This choice was taken in light of the work in Ref. 6, which showed that the CO serves primarily as an agent to keep the reaction going and is not an important component of the critical fluctuations. In the O saturated state this order parameter obviously vanishes, and near the transition point $y_1$ in an infinite system we expect a dependence of the form

$$\psi(y_{CO}) \propto (y_{CO} - y_1)^{\beta} . \tag{1}$$

We assume that near the second-order transition that $\psi$ obeys a finite-size scaling form

$$\psi(y_{CO}, L) = L^{-\beta/\nu} F(|y_{CO} - y_1| L^{1/\nu}) , \tag{2}$$

where $\nu$ measures the growth of the correlation length $\xi$, near the transition $\xi \propto |y_{CO} - y_1|^{\nu}$, and $F(x) \propto x^{\beta}$ for large $x$ so that Eq. (1) obtains for $L \to \infty$.

We also calculated the dynamical exponent $z$ by finite-size scaling, where $z$ describes the critical slowing down of the fluctuations near the transition. If $\tau$ measures the time scale for relaxation, we expect

$$\tau \propto \xi^z \propto |y_{CO} - y_1|^{z\nu} . \tag{3}$$

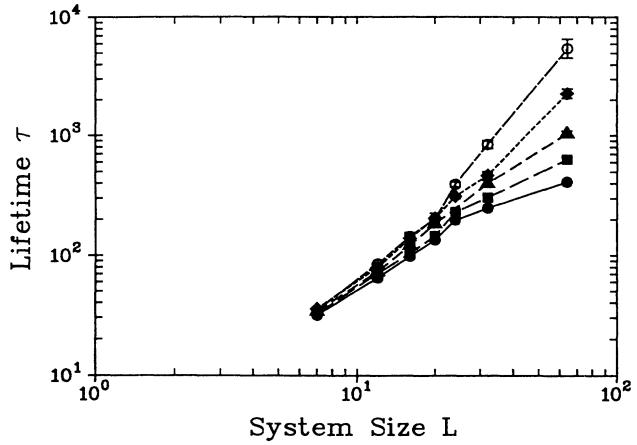


FIG. 6. The mean lifetime $\tau$ as defined in Eq. (4) vs system size $L$ for various choices of $y_{CO}$. The symbols for various $y_{CO}$ are $y_{CO} = 0.426$, solid circles; $y_{CO} = 0.428$, squares; $y_{CO} = 0.430$, triangles; $y_{CO} = 0.432$, diamonds; and $y_{CO} = 0.434$, circles. The straightest curve yields a value of $y_1 = 0.430$.

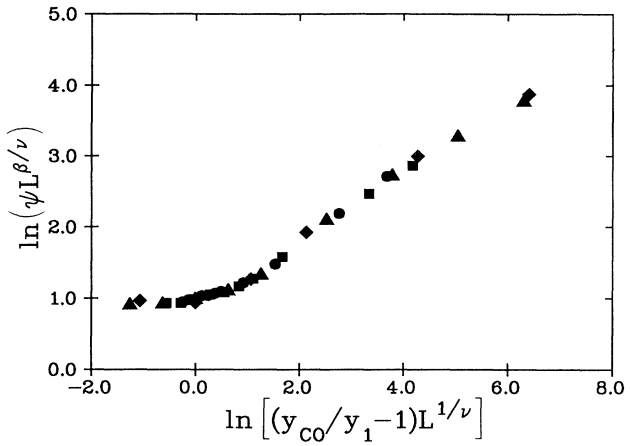


FIG. 7. Scaling plot of $\ln(\psi L^{\beta/\nu})$ vs $\ln(|y_{CO}/y_1 - 1|L^{1/\nu})$ for various system sizes with $R_x = 0.2$. The fact that all the data collapse onto a single curve justifies the scaling relationship postulated in Eq. (4). The symbols for the different system sizes are $L = 40$, circles; $L = 64$, squares; $L = 80$, triangles; and $L = 100$, diamonds.

For our simulations, we define a characteristic time $\tau$ for the system to become poisoned[19] as

$$\tau = \frac{\sum_t t\ \psi(t)}{\sum_t \psi(t)}\ , \tag{4}$$

where the sum is over the simulation time in MCS and $\psi(t)$ is the number of sites not occupied by oxygen atoms at time $t$. Below $y_1$, we expect $\tau$ will grow exponentially with the system size, while above $y_1$ we expect $\tau$ to have the finite-size scaling form

$$\tau(y_{CO}, L) = L^z G(|y_{CO} - y_1|L^{1/\nu})\ , \tag{5}$$

where $G(x) \propto x^{-z\nu}$ for large $x$.

The simulations for the finite-size scaling analysis were done using a variety of lattice sizes, from 7×7 to 100×100, starting with an empty lattice and sampling the state of the system regularly until the surface was saturated. The average of these samples gave the values of $\psi$ and $\tau$ for that run. For each $L$, we made several hundred independent runs and averaged $\psi$ and $\tau$ to find the characteristic values for the given lattice size.

From Eq. (2), $\psi$ is proportional to $L^{-\beta/\nu}$ at the critical point $y_1$. A log-log plot of $\psi$ versus $L$ at $y_1$ should give a straight line with slope $-\beta/\nu$. Similarly, a log-log plot of $\tau$ versus $L$ at $y_1$ should give a straight line with slope $z$. In Fig. 6, we plot $\ln(\tau)$ versus ln(L) for $L$=7, 12, 16, 20, 24, 32, and 64 for $R_x$=0.2. We determined the value of $y_{CO}$ from the $\ln(\tau)$ versus $\ln(L)$ graph since its curvature is more sensitive to value of $y_1$ than the plot $\ln(\psi)$ versus $\ln(L)$ in the critical region, and thus gives a more accurate determination of $y_1$. We have therefore omitted a plot of $\psi$ versus $L$, but we stress that the two values of $y_1$ determined from both the static and dynamic scaling analysis are consistent.

If $\psi L^{\beta/\nu}$ is plotted against $|y_{CO} - y_1|L^{1/\nu}$, curves with different $L$ values should collapse to a single curve for the correct choice for $\beta$ and $\nu$. Our results are shown in Fig. 7, which shows data from $L$=16, 32, 64, and 100 on a single curve. Table I lists the values for $\beta$ and $\nu$ determined in this manner for three different choices of $R_x$. The error bars for $\beta$ are determined by varying $\beta$ until the curves fail to collapse well to the eye. Similarly, if $\tau L^{-z}$ is plotted against $|y_{CO} - y_1|L^{1/\nu}$, curves with different $L$ values should collapse to a single curve. We collapsed data with $L$=40, 64, 80, and 100 onto a single curve with fixed $\nu$. Table II gives the values of $\nu$ obtained in this fashion. The error bars for $\nu$ are obtained in the similar fashion as for $\beta$. As we observe, the value of $\nu$ obtained by two different methods are consistent within the error bars. We should point out that the curve for $R_x$=0.70 does not collapse as well as for smaller values of $R_x$. We suspect that the finite-size scaling assumption

TABLE I. Critical behavior deduced from static scaling for various amounts of anisotropy.

| $R_x$ | $y_1$ | $\beta/\nu$ | $\beta$ | $\nu$ |
|---|---|---|---|---|
| 0.70 | 0.196 ± 0.002 | 0.75 ± 0.02 | 0.59 ± 0.02 | 0.74 ± 0.04 |
| 0.50 | 0.332 ± 0.001 | 0.77 ± 0.01 | 0.65 ± 0.06 | 0.82 ± 0.07 |
| 0.20 | 0.4305 ± 0.0005 | 0.78 ± 0.01 | 0.64 ± 0.04 | 0.83 ± 0.05 |

TABLE II. Critical behavior from dynamical scaling for various amounts of anisotropy.

| $R_x$ | $y_1$ | $\nu$ | $z$ |
|---|---|---|---|
| 0.70 | $0.196 \pm 0.002$ | $0.64 \pm 0.14$ | $1.70 \pm 0.06$ |
| 0.50 | $0.332 \pm 0.001$ | $0.70 \pm 0.10$ | $1.67 \pm 0.06$ |
| 0.20 | $0.4305 \pm 0.0005$ | $0.75 \pm 0.10$ | $1.64 \pm 0.03$ |

is only approximately valid there due to the fact that $R_x$ is close to the value of 0.742 at which second-order transition disappears.

We believe that our model belongs to the directed percolation universality class,[7,9,11] even though the critical exponent $\beta$ is consistently larger than the value of 0.58 found for directed percolation in (2+1) dimensions.[8] The reason we believe this is that if one examines the $\beta/\nu$ values for various $R_x$, they are all roughly 0.77, which is the value of $\beta/\nu$ for (2+1)-dimensional directed percolation.[9] We suspect that our value of $\beta$ is larger than that found in directed percolation because of systematic errors in determining $\nu$ from the collapsing of the data for different $L$. This collapsing process also requires a good estimate of $y_1$, while $\beta/\nu$ is less sensitive to our determination of $y_1$. We have no independent way of calculating $\nu$ other than to infer it by collapsing the data, so we cannot rule out systematic error. Therefore we believe $\beta/\nu$ is a much better indicator than $\beta$ itself. Further evidence that suggests directed percolation comes from the dynamical exponent $z$, which agrees with the directed percolation value of 1.69.[9]

## IV. CONCLUSION

We have studied here a kinetic model for CO oxidation on an anisotropic catalytic surface. This model exhibits transitions similar to those seen in the ZGB model. However, in this model the second-order critical point varies as a function of reaction rate $R_x$, and can actually disappear if $R_x$ is large enough, while the first-order transition point is almost unaffected. For $R_x \equiv 1$, the reactive steady state is replaced by a saturated surface of random rows of pure O or pure CO. Diffusion changes the phase diagram only when the diffusion rate exceeds the reaction rate. It affects primarily the first-order transition by shifting the transition point to larger $y_{CO}$ and reducing the jump in concentration.

From a finite-size scaling analysis, we obtained the critical exponents $\beta$, $\nu$, and $\tau$ for various degrees of anisotropy. Our results indicate that spatial anisotropy, just as in case of an equilibrium system, does not affect the critical behavior of a nonequilibrium system. Furthermore, our results suggest that this model belongs to the universality class of Reggeon field theory and directly percolation, which lends support to the hypothesis that the critical behavior in any transition to a noiseless state should be in the Reggeon field theory universality class.[7,10]

## ACKNOWLEDGMENTS

B. Y. and D. A. B. would like to thank the Laboratory of Surface Science and Technology at the University of Maine, where portions of this work were done, for their hospitality.

[1] S.-K. Ma, Rev. Mod. Phys. **45**, 589 (1973); K. G. Wilson, *ibid.* **47**, 773 (1975).
[2] R. Kopelman, S. Parus, and J. Prasad, Phys. Rev. Lett. **56**, 1742 (1986); J. Prasad and R. Kopelman, *ibid.* **59**, 2103 (1987).
[3] G. Nicolis and I. Prigogine, *Self Organization in Nonequilibrium Systems* (Wiley, New York 1977).
[4] R. M. Ziff, E. Gulari, and Y. Barshad, Phys. Rev. Lett. **56**, 2553 (1986).
[5] R. Dickman, Phys. Rev. A **34**, 4624 (1986).
[6] P. Meakin and D. Scalapino, J. Chem. Phys. **96**, 731 (1919).
[7] G. Grinstein, Z.-W. Lai, and D. A. Browne, Phys. Rev. A **40**, 4820 (1989).
[8] H. D. I. Abarbanel, J. B. Bronzan, R. L. Sugar, and A. R. White, Phys. Rep. C **12**, 120 (1975).
[9] W. Kinzel, Ann. Israel Phys. Soc. **5**, 425 (1983); J. L. Cardy and R. L. Sugar, J. Phys. A **13**, L423 (1980); R. C. Brower, M. A. Furman, and M. Moshe, Phys. Lett. B **76**, 213 (1978). The critical exponents in these papers are defined differently from the usual convention. If the exponents in these papers are denoted with primes, the conversion is $z = z'\nu'/2$.
[10] H. K. Janssen, Z. Phys. B **42**, 151 (1981); P. Grassberger, *ibid.* **47**, 365 (1982).
[11] I. Jensen, H. C. Fogedby, and R. Dickman, Phys. Rev. A **41**, 3411 (1990).
[12] M. Dumont, M. Poriaux, and R. Dagonnier, Surf. Sci. **169**, L307 (1986).
[13] P. Araya, W. Porod, R. Sant, and E. E. Wolf, Surf. Sci. **208**, L80 (1989).
[14] M. Ehsasi, M. Matloch, O. Frank, J. H. Block, K. Christmann, F. S. Rys, and W. Hirschwald, J. Chem. Phys. **91**, 4949 (1989).
[15] H.-P. Kaukonen and R. M. Nieminen, J. Chem. Phys. **91**, 4380 (1989).
[16] M. Silverberg, A. Ben-Shaul, and F. Rebentrost, J. Chem. Phys. **83**, 6501 (1985).
[17] T. Engel and G. Ertl, *The Chemical Physics of Solid Surfaces and Heterogeneous Catalysis*, edited by D. A. King and D. P. Woodruff (Elsevier, Amsterdam, 1982), Vol. 4, p. 92.
[18] P. Flory, J. Am. Chem. Soc. **61**, 1518 (1939).
[19] T. Aukrust, D. A. Browne, and I. Webman, Europhys. Lett. **10**, 249 (1989); Phys. Rev. A **41**, 5301 (1990).